

Additive-assisted synthesis and optoelectronic properties of $(\text{CH}_3\text{NH}_3)_4\text{Bi}_6\text{I}_{22}$

*Manila Sharma,¹ Aymen Yangui,¹ Alain Lusso,² Kamel Boukhedden,² Xiixin Ding,⁴ Mao-Hua Du,³
Krzysztof Gofryk,⁴ Bayrammurad Saparov^{1*}*

¹Department of Chemistry and Biochemistry, University of Oklahoma, 101 Stephenson Parkway, Norman, Oklahoma 73019, United States

²Groupe d'Étude de la Matière Condensée, CNRS-UMR8635, Université de Versailles Saint Quentin, Université Paris-Saclay, 45 Avenue des États-Unis, 78035 Versailles cedex, France.

³Materials Science and Technology Division, Oak Ridge National Laboratory, Oak Ridge, TN 37831, USA

⁴Idaho National Laboratory, Idaho Falls, ID 83415, USA

Supporting Information

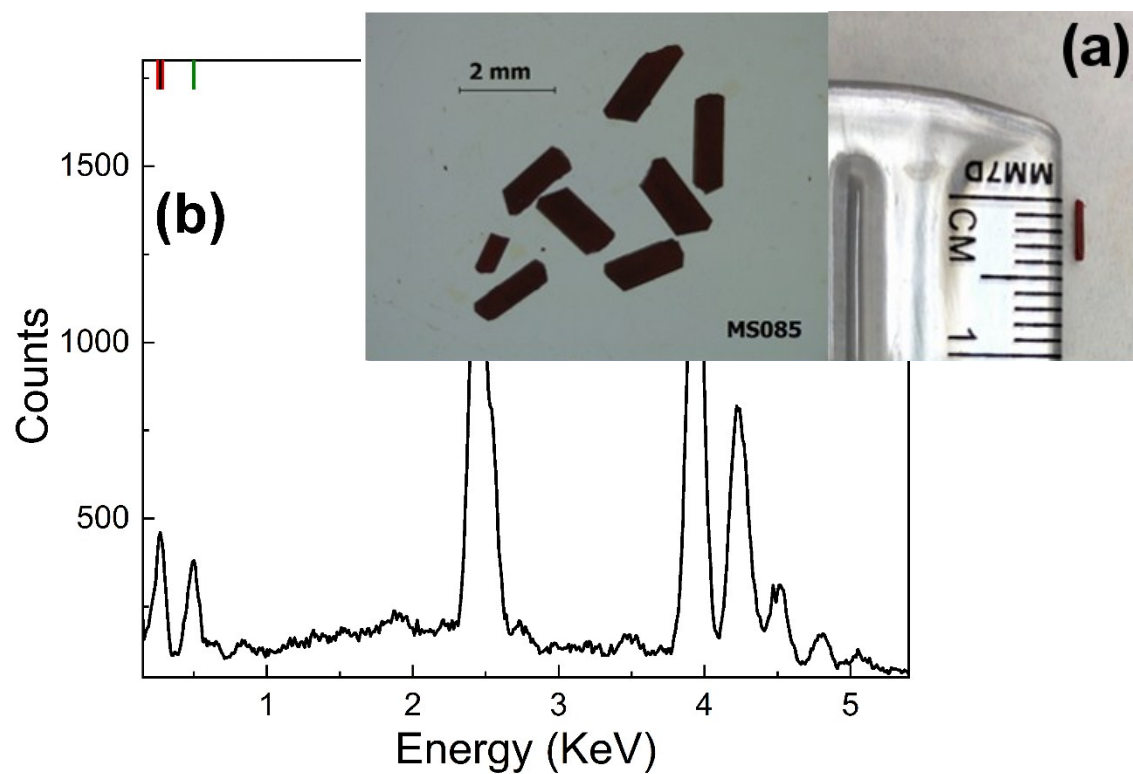


Figure S1. (a) An optical image of as-prepared deep red crystals of $(MA)_4Bi_6I_{22}$. (b) A typical energy-dispersive X-ray (EDX) spectrum for a $(MA)_4Bi_6I_{22}$ crystal.

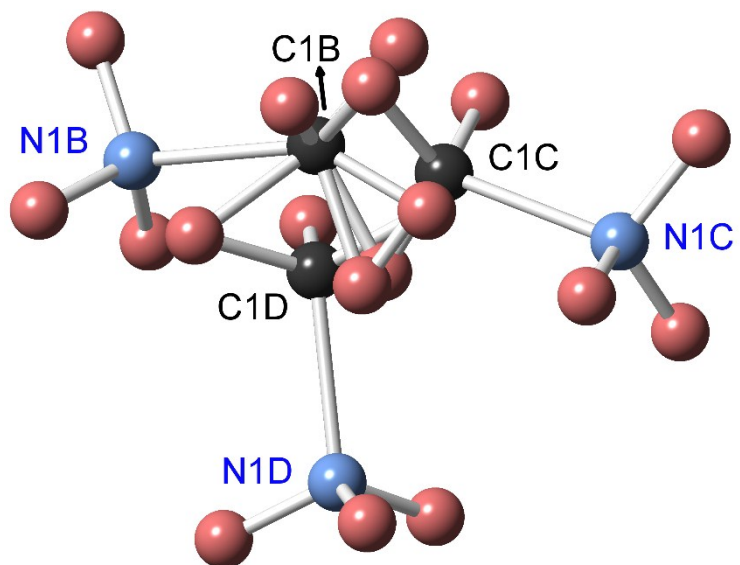


Figure S2. Rotational disorder in methylammonium cation in $(\text{MA})_4\text{Bi}_6\text{I}_{22}$.

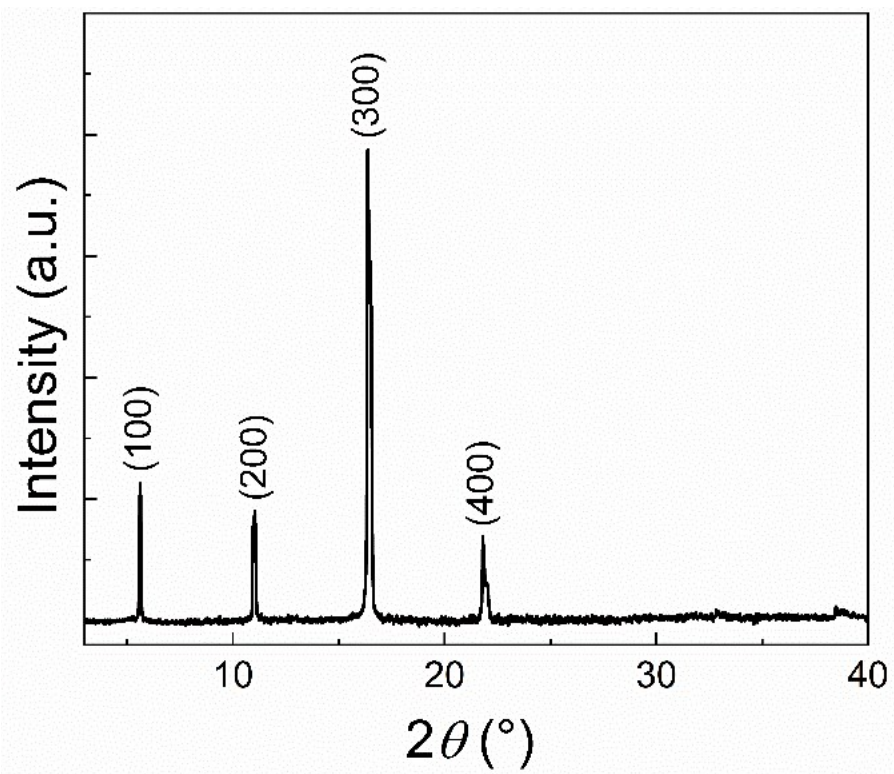


Figure S3. An experimental XRD pattern measured for a single crystal of $(\text{MA})_4\text{Bi}_6\text{I}_{22}$ at room temperature.

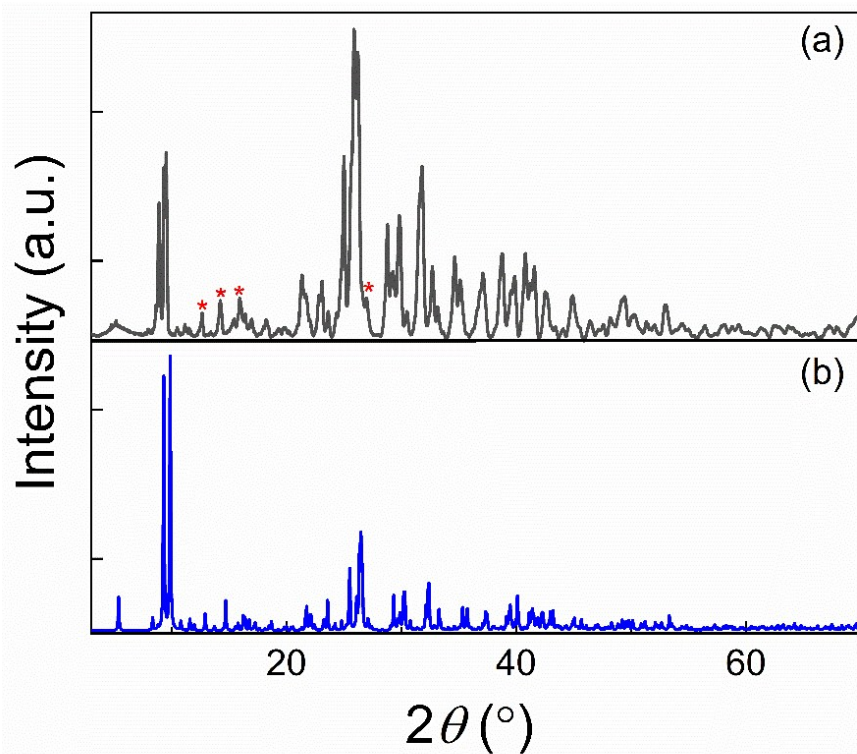


Figure S4. (a) Upon grinding $(\text{MA})_4\text{Bi}_6\text{I}_{22}$ single crystals, an emergence of BiI_3 impurity peaks (masked with red stars) is clearly noticeable in PXRD patterns. (b) The simulated PXRD pattern for $(\text{MA})_4\text{Bi}_6\text{I}_{22}$.

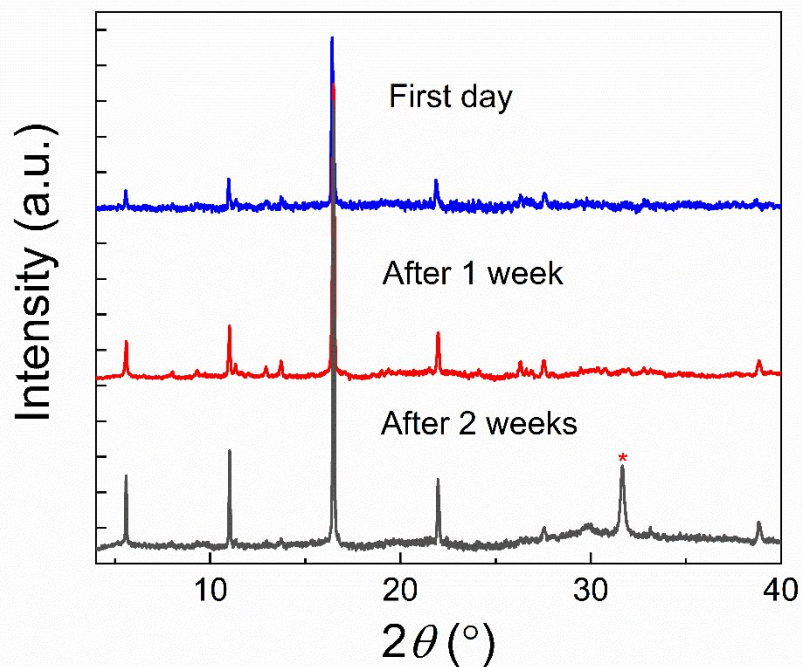


Figure S5. PXR D patterns of as-prepared crystals (blue) of $(\text{MA})_4\text{Bi}_6\text{I}_{22}$, and after 1 week (red) and 2 weeks (black) exposure to ambient air. After 2 weeks, appearance of an impurity peak (most likely BiOI, marked with a red star) is noticeable.

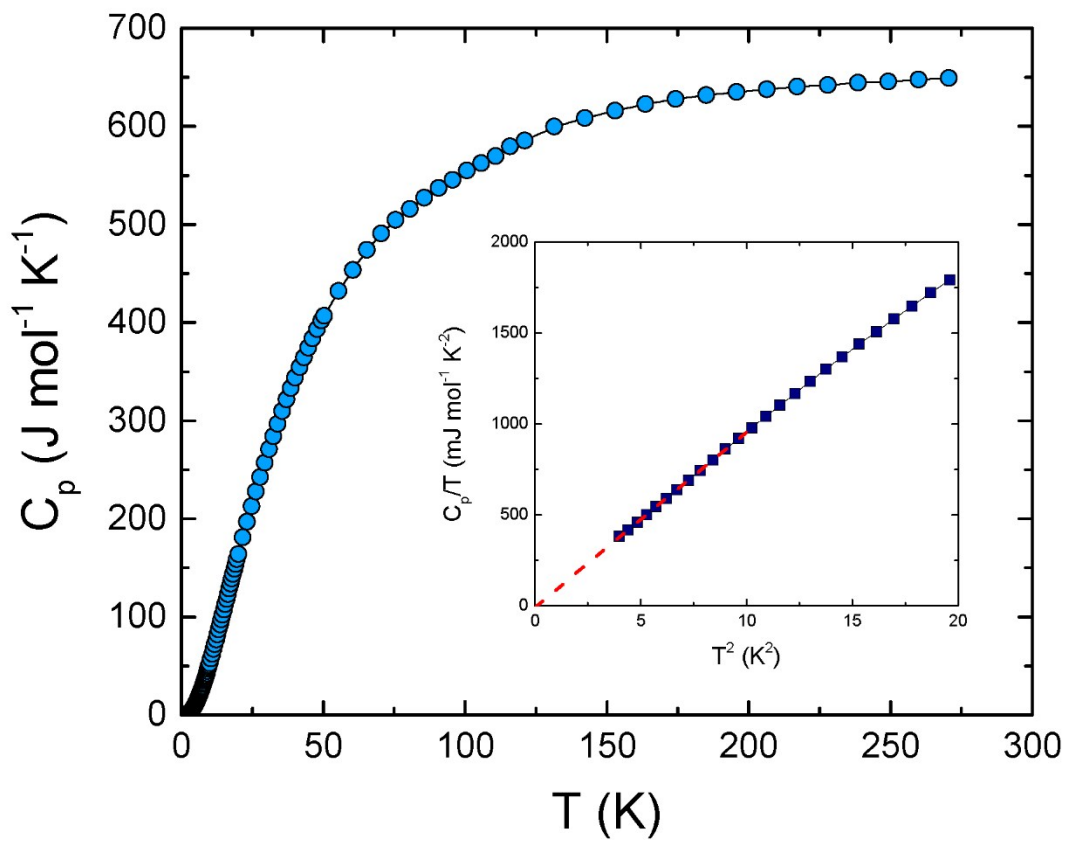


Figure S6. The temperature dependence of specific heat for $(\text{MA})_4\text{Bi}_6\text{I}_{22}$. The inset shows plot of C/T vs T^2 .

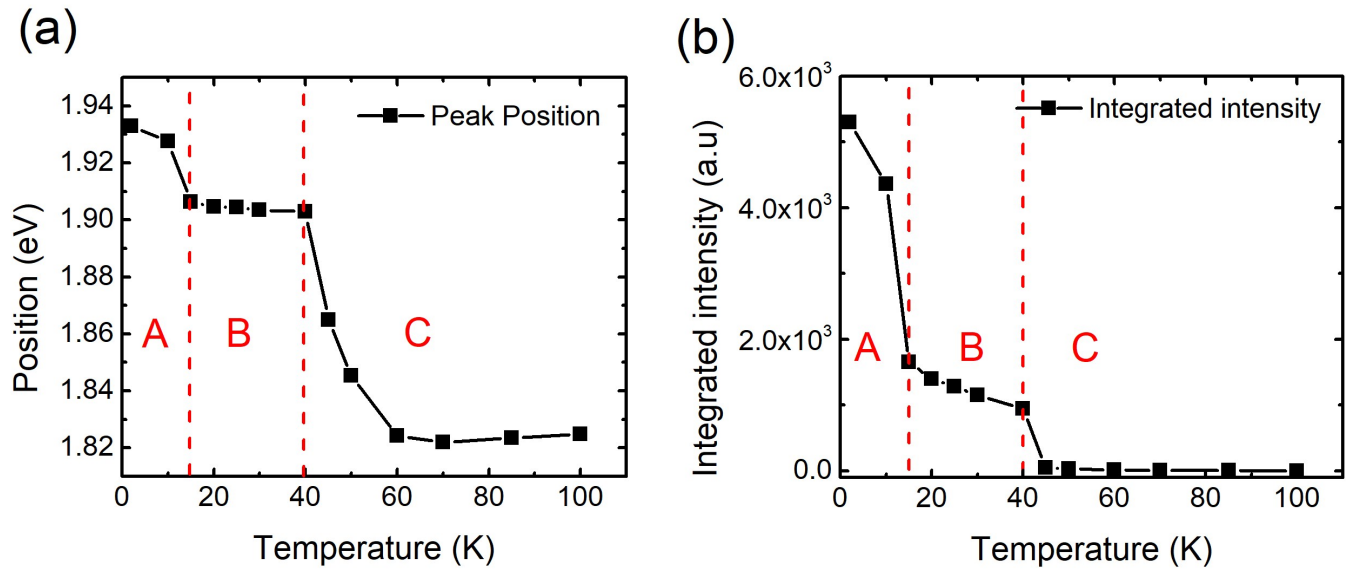


Figure. S7. Temperature dependence of (a) PL peak position and (b) integrated PL intensity. Dashed lines highlight the presence of three different regimes noted A, B, and C.

Table S1. Selected interatomic distances (Å) and angles (°) in (MA)₄Bi₆I₂₂.

Label		Distance	Label	Angle
Bi1-	I1	2.9622(6)	I1-Bi1-I2	94.39(2)
	I2	2.9273(8)	I2-Bi1-I5	87.31(2)
	I3	2.8623(7)	I1-Bi1-I5	173.431(18)
	I4	3.2546(7)	I2-Bi1-I4	172.27(2)
	I5	3.2528(6)		
	I7	3.4161(6)		
Bi2-	I4	3.2433(6)	I4-Bi2-I5	89.694(17)
	I4	3.3840(6)	I5-Bi2-I8	90.849((18)
	I5	3.0369(7)	I4-Bi2-I8	172.871(17)
	I6	2.8522(6)	I5-Bi2-I7	172.470(17)
	I7	3.1596(7)		
	I8	2.9618(6)		
Bi3-	I1	3.3957(7)	I7-Bi3-I8	82.790(16)
	I7	3.3640(6)	I8-Bi3-I11	92.925(19)
	I8	3.3717(7)	I7-Bi3-I11	168.412(17)
	I9	2.8873(7)	I8-Bi3-I10	170.987(18)
	I10	2.8788(7)		
	I11	2.8813(6)		